DOI:
10.1016/j.jorganchem.2015.09.032

Document Version
Peer reviewed version

Oxidative-addition of the N–H bond of saccharin (sacH) to a triosmium centre: Synthesis, structure and reactivity of $Os_3(CO)_{10}(\mu\text{-}H)(\mu\text{-}sac)$[1]

Shirajum Monira[a], Sadiya Afrin[a], Kazi A. Azam[a,*], Md. Kamal Hossain[a], Derek A. Tocher[b], Shishir Ghosh[a], Subas Rajbangshi[a], Shariff E. Kabir[a], Graeme Hogarth*[c]

[a] *Department of Chemistry, Jahangirnagar University, Savar, Dhaka 1342, Bangladesh*

[b] *Department of Chemistry, University College London, 20 Gordon Street, London WC1H OAJ, UK*

[c] *Department of Chemistry, King's College London, Britannia House, 7 Trinity Street, London SE1 1DB, UK*

* Corresponding authors.

E-mail address: kazi.ali.azam@gmail.com (K.A.Azam); graeme.hogarth@kcl.ac.uk (G. Hogarth)

ABSTRACT

Saccharin (sacH) is a widely-used sweetener and consequently its chemistry has been extensively studied, but here we report a rare example of its reactivity towards a multinuclear metal centre. Lightly-stabilized $Os_3(CO)_{10-n}(NCMe)_n$ (n = 1, 2) react with sacH to afford $Os_3(CO)_{10}(\mu\text{-}H)(\mu\text{-}sac)$ (**1**) in which the sac ligand bridges an osmium-osmium vector *via* nitrogen and the carbonylic oxygen (μ-N,O). The reactivity of **1** towards monodentate phosphines, PR_3 (R = Ph, Th, Fu), has been investigated. Carbonyl substitution affords both mono- and bis-phosphine substituted derivatives $Os_3(CO)_9(PR_3)(\mu\text{-}H)(\mu\text{-}sac)$ (**2**) and $Os_3(CO)_8(PR_3)_2(\mu\text{-}H)(\mu\text{-}sac)$ (**3**) respectively. In the mono-substituted derivatives, the phosphine occupies an equatorial position on the osmium that is directly bonded to the carbonylic oxygen of saccharinate, while in the bis-(phosphine) substituted derivatives the second phosphine is bound to the remote osmium also occupying an equatorial site. In all complexes the saccharinate ligand remains in the bidentate N,O coordination mode thus playing a directing spectator role in these reactions.

[1] This paper is dedicated to Professor Kazi Azam on the occasion of his retirement. A talented scientist, true gentleman, and inspiration to generations of students at Jahangirnager University.

***Keywords*:** Triosmium clusters; Carbonyls; Saccharin; N–H bond activation; X-ray structures

1. Introduction

Saccharin (sacH) and its water soluble saccharinate salts are the most widely used artificial sweeteners [1], the latter being formed easily due to acidic nature of the imido hydrogen. The coordination chemistry of the sac has been extensively investigated revealing its versatile coordination properties as it possesses four donor atoms to bind with transition metal centres – one nitrogen and three oxygens (one carbonylic and two sulfonic) [2]. Although it can bind to transition metals in a number of different ways using these donor atoms, the simple N-bound coordination (**I** in Chart 1) is by far the most commonly observed [2,3].

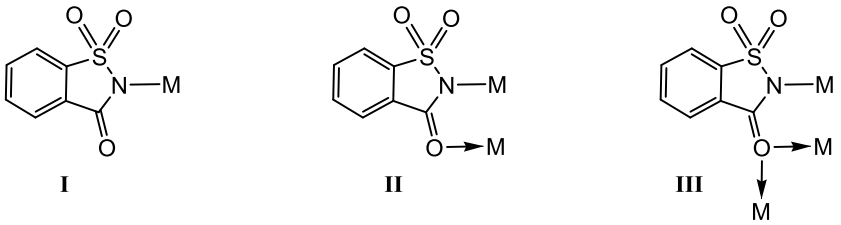

Chart 1.

The organometallic chemistry of the sac has been relatively neglected and only a few organometallic sac complexes are known [4-8]. In 1987, Beck and co-workers reported sac complexes of the Group VI metal carbonyls Na[$M(CO)_5(\kappa^1$-(N)-sac)] from the reactions of $M(CO)_5$(thf) and Na(sac) [8]. More recently, Süss-Fink and co-workers reported a series of η^6-arene complexes, (η^6-arene)$Ru(\kappa^1$-(N)-sac$)_2$(L) (L = H_2O, CH_3CN), synthesized from [(η^6-arene)$RuCl_2]_2$ and Na(sac) in a 1:1 mixture of water-ethanol or acetonitrile-methanol [7]. These half-sandwich ruthenium complexes were found to catalyze the oxidation of secondary alcohols to the corresponding ketones in presence of *tert*-butyl hydroperoxide in aqueous medium [7].

As far as we are aware, there is only one previous example of the reactions of saccharin with low valent cluster centres. In 2006, Buck and Mass reported the formation of di- and tetra-ruthenium complexes, $Ru_2(CO)_6(\mu$-sac$)_2$ (**A**) and [$Ru_2(CO)_6(\mu$-sac$)_2]_2$ (**B**) respectively, from reactions of $Ru_3(CO)_{12}$ and excess saccharin at elevated temperatures (Scheme 1) [4]. In

binuclear **A**, both sac ligand bridge the two ruthenium centres using nitrogen and the carbonylic oxygen (**II** in Chart 1) in a head-tail fashion, whereas a head-head arrangement of sac ligands are observed in **B** with two of them now bonded to ruthenium centres in triply-bridging fashion (**III** in Chart 1) using the same donor atoms. Both of these complexes undergo axial carbonyl substitution in the presence of 2-electron donor ligands to give substituted diruthenium complexes [4]. Further, **A** and **B** are suitable pre-catalysts for the cyclopropanation of nucleophilic alkenes with methyl diazoacetate [4], the later has also been found to catalyze the intramolecular carbenoid C–H insertion of α-diazo esters leading to the formation of β- and/or γ-lactams [5,6].

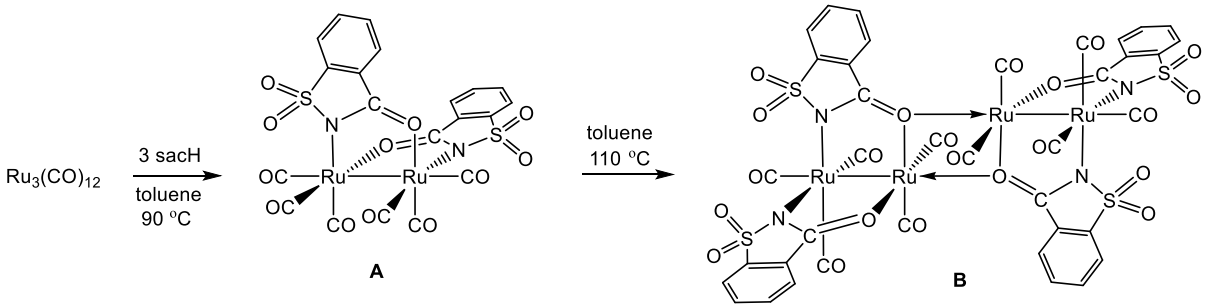

Scheme 1. Reaction of $Ru_3(CO)_{12}$ with sacH

The triply-bridging coordination mode of the sac ligand observed in **B** indicates that it can, in principle, bind to a trinuclear centre in a capping fashion. Reaction of $Ru_3(CO)_{12}$ with saccharin only takes place at elevated temperatures and under these forcing conditions breakdown of the tri-nuclear framework occurs. To prevent this and with the aim of investigating the coordination chemistry of the sac ligand at a trinuclear center we have now investigated the reaction of lightly-stabilized $Os_3(CO)_{10n}(NCMe)_n$ (n = 1, 2) with saccharin which resulted in the formation of trinuclear $Os_3(CO)_{10}(\mu\text{-H})(\mu\text{-sac})$ (**1**) *via* oxidative-addition of N–H bond. The reactivity of this sac-bridged triosmium cluster towards various monodentate phosphines has also been investigated.

2. Results and discussion

2.1. Reactions of $Os_3(CO)_{10-n}(NCMe)_n$ (n = 1, 2) with saccharin: Oxidative-addition of N–H bond at triosmium centres

In early 1980s, Johnson and Lewis investigated the reactivity of $Os_3(CO)_{10}(NCMe)_2$ towards acyclic amides, $RCONH_2$ (R = H, Me, Et, Pr, Ph) [9], N-H oxidative-addition resulting in formation of $Os_3(CO)_{10}(\mu\text{-}H)(\mu\text{-}HNCOR)$, which were characterized on the on the basis of spectroscopic data [9]. The cyclic amide saccharin (sacH) likewise reacts with $Os_3(CO)_{10}(NCMe)_2$ under similar conditions. Thus heating a benzene solution of $Os_3(CO)_{10-n}(NCMe)_n$ (n = 1, 2) with saccharin at 80 °C led to the isolation of $Os_3(CO)_{10}(\mu\text{-}H)(\mu\text{-}sac)$ (**1**) in moderate to good yields (34%, n = 1; 61%, n = 2), after chromatographic separation and work-up (Scheme 2). Cluster **1** is formed by oxidative-addition of the N–H bond of saccharin to the parent cluster accompanied by coordination of the carbonylic oxygen to an adjacent osmium.

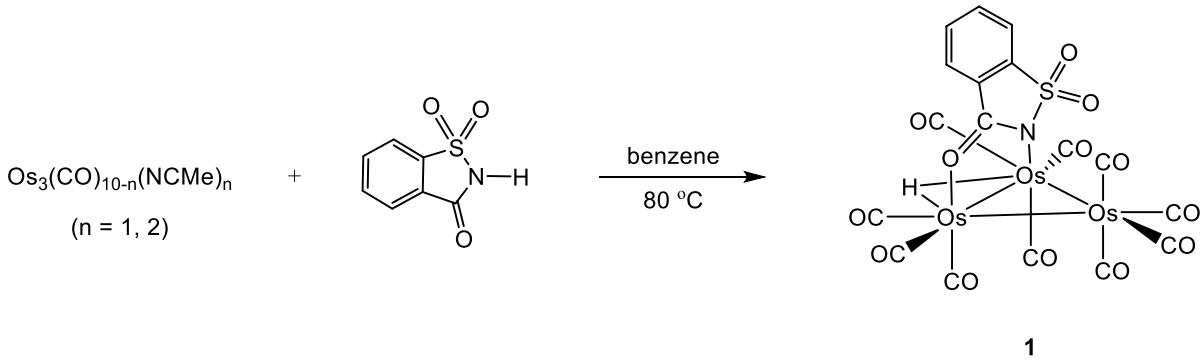

Scheme 2. Synthesis of $Os_3(CO)_{10}(\mu\text{-}H)(\mu\text{-}sac)$ (**1**)

Cluster **1** has been characterized by a combination of analytical and spectroscopic data together with single crystal X-ray diffraction analysis. An ORTEP diagram of the molecular structure of **1** is depicted in Fig. 1 with the caption containing selected interatomic distances and angles. The cluster core consists of an approximate isosceles triangle of osmium metals [Os(1)–Os(2) 2.9224(3), Os(1)–Os(3) 2.8730(3) and Os(2)–Os(3) 2.8934(3) Å] coordinated by ten carbonyls and a sac and hydride ligands. Both the sac ligand and hydride act in bridging capacity and span across the longest osmium-osmium edge. The sac ligand uses its nitrogen and carbonylic oxygen for bonding with the cluster core thus serving as a three electron donor. It bridges the Os(1)–Os(2) edge by coordinating to these osmium metals through one of their axial coordination sites and lies almost perpendicular to the metallic plane. The bridging hydride was located from a Fourier map which lies approximately within the metallic plane. This type of bridging coordination mode of sac ligand is not very common. It has previously been observed in di- and tetra-ruthenium complexes **A**-**B** (Scheme 1) [4], in dinuclear copper complexes $[Cu(PPh_3)(\mu\text{-}sac)]_2$ [10] and $[Cu(\kappa^1\text{-(N)-imidazole})_2(\kappa^1\text{-}sac)(\mu\text{-}sac)]_2$ [11], in dinuclear palladium complexes $[Pd(\kappa^2\text{-L})(\mu\text{-}sac)]_2$ (L = 2-(2-

pyridyl)phenyl, 7,8-benzoquinolyl) [12] and dinuclear chromium complexes of the type $[Cr(\mu\text{-sac})_2]_2$ or $[Cr(\mu\text{-sac})_2L]_2$ [13]. Among the ten terminal carbonyls, four are bonded to the remote osmium, Os(3), while the rest are evenly distributed between Os(1) and Os(2). The Os–N [2.149(4) Å] [14-16] and Os–O [2.134(4) Å] [17] bond distances are very similar to those reported for related clusters. Spectroscopic data show that the solid-state structure persists in solution. The ^{1}H NMR spectrum of **1** displays a high field singlet at δ –11.61 assigned to the bridging hydride, in addition to resonances in the aromatic region for the sac ligand protons. The carbonyl stretching of the sac ligand appears at 1672 cm^{-1} for **1** as compared to that of free saccharin (1726 cm^{-1}), the red shift indicating that the C=O bond becomes weaker upon coordination to the triosmium centre, and this is in accord with the lengthening of the C=O bond distance in **1** [1.255(6) Å] as compared to that in free saccharin [1.214(5) Å] [18].

Reactions of $Os_3(CO)_{10-n}(NCMe)_n$ (n = 1, 2) with saccharin took *ca.* 48 h for completion when conducted at room temperature in CH_2Cl_2 and gave **1** in *ca.* 15-20% yield. A second band was also observed by TLC from the reaction of $Os_3(CO)_{11}(NCMe)$. This product shows the highest energy absorption at 2145 cm^{-1} in the carbonyl region of the IR spectrum (2145m, 2100vs, 2077vs, 2069s, 2058s, 2037s, 2016s, 1996m cm^{-1}) as compared to the highest energy absorption of **1** at 2115 cm^{-1} indicating that it may be a $(CO)_{11}$ cluster. The hydride region of the ^{1}H NMR spectrum of this second product shows two singlets at δ –16.96 and –15.81 in 2:1 ratio. This suggests that it contains a bridging hydride and is fluxional in solution most probably due to migration of this hydride across different osmium-osmium edges. However, we could not grow single crystals for X-ray diffraction since this cluster slowly converted to **1** in solution during crystallization. From the IR and ^{1}H NMR spectroscopic data, we assume that the reactions of saccharin with these lightly stabilized clusters commence with oxidative-addition of the N–H bond *via* formation of $Os_3(CO)_{11}(\mu\text{-H})(\kappa^1\text{-sac})$ as shown in Scheme 3.

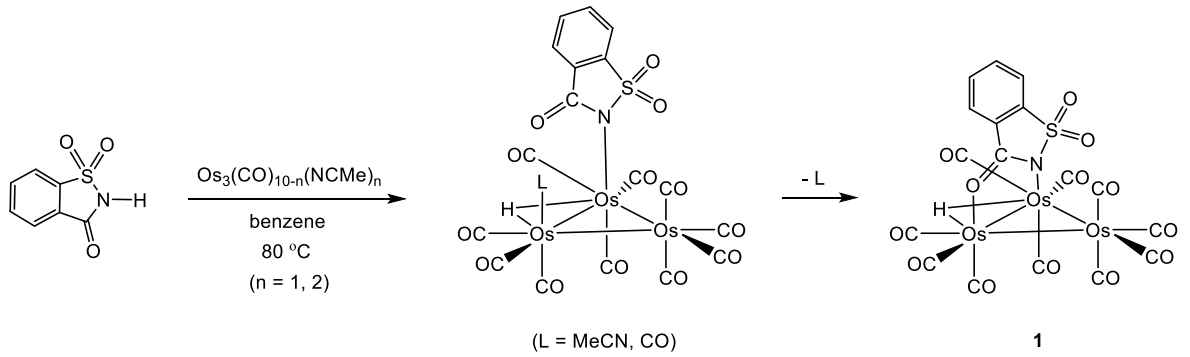

Scheme 3. Proposed route for the formation of $Os_3(CO)_{10}(\mu\text{-}H)(\mu\text{-}sac)$ (**1**) *via* $Os_3(CO)_{11}(\mu\text{-}H)(\kappa^1\text{-}sac)$

*2.2. Reactions of **1** with PR_3: Carbonyl substitution by phosphines*

We have recently compared the relative reactivity and coordination behaviour of PPh_3, PTh_3 and PFu_3 in a range of chemical systems [19-22] since although PTh_3 and PFu_3 are sterically quite similar to the widely-utilized PPh_3 ligand, the electron-withdrawing nature of the thienyl and furyl rings is significantly greater than that of the phenyl ring which makes these hetero-difunctional phosphines poorer σ-donors than PPh_3 [23]. These subtle electronic differences can potentially be utilized to prepare more efficient catalysts for certain catalytic transformations and also to gain insight into key mechanistic transformations [24,25]. Here we have studied the reactions of **1** with these three phosphines. Thermal treatment of **1** in presence of two equivalent PR_3 in boiling toluene led to the formation of mono- and bis-(phosphine) substituted derivatives $Os_3(CO)_9(PR_3)(\mu\text{-}H)(\mu\text{-}sac)$ (**2**) and $Os_3(CO)_8(PR_3)_2(\mu\text{-}H)(\mu\text{-}sac)$ (**3**), respectively, in moderate to good yields (Scheme 4).

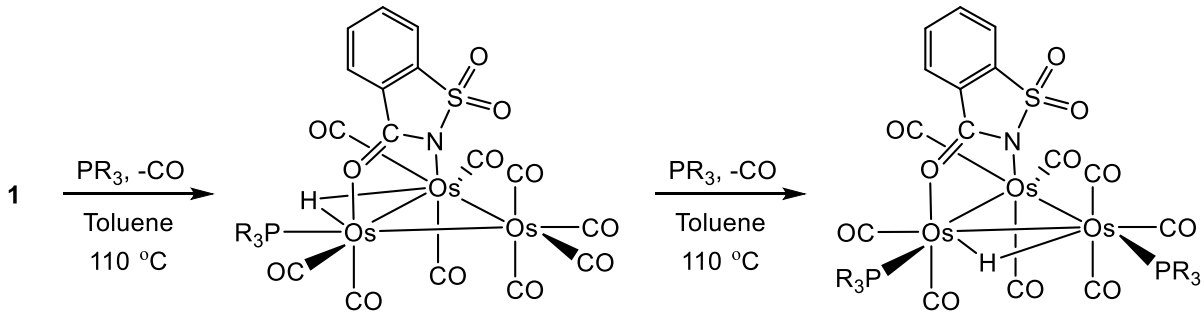

2a, R = Ph
2b, R = Th
2c, R = Fu

3a, R = Ph
3b, R = Th
3c, R = Fu

Scheme 4. Reactions of $Os_3(CO)_{10}(\mu\text{-}H)(\mu\text{-}sac)$ (**1**) with various monodentate phosphines

All three mono-(phosphine) substituted derivatives **2a-c** have been characterized by single crystal X-ray diffraction analysis the results of which are summarized in Figs. 2-4 and Table 1. There are two independent molecules in the asymmetric unit of **2c** but only of one of these is shown in Fig. 4 since they exhibit no significant structural differences. Figs. 2-4 show that

2a-c are structurally similar and their overall structures are also very similar to that of the parent cluster **1** except that one of the equatorial carbonyls on the carbonylic oxygen bound osmium have been replaced by a phosphine. Phosphine coordination at the oxygen-bound iron rather than carbon-bound iron has been noted earlier in diiron-acyl complexes [20]. Thus the oxygen-bound metal center is relatively electron-deficient, as compared to nitrogen- or carbon-bound metal center(s), as this electronic factor probably directs carbonyl substitution by a more σ-donating phosphine to take place at oxygen-bound metal center in these complexes. Akin to **1**, the osmium metals forms an isosceles triangle with two short and one relatively long osmium-osmium edges in all of them (Table 1). In a similar fashion, the longest edge of the metal triangle is simultaneously bridged by the sac and hydride ligands with the sac ligand lying almost perpendicular to the metallic plane. The Os–N and Os–O bond distances observed in these clusters are almost identical within the experimental error with that of **1** (Table 1). The Os–P bond distance found in **2b** and **2c** are slightly shorter (*ca.* 0.03 Å) than that of **2a** which is expected since PTh_3 and PFu_3 are better π-acceptors than PPh_3 [23]. The hydride was located from a Fourier map for **2a** and **2c** and found to lie *cis* to phosphine within the metallic plane. The spectroscopic data for **2a-c** suggest that they retain their solid-state structure in solution. The $^{31}P\{^{1}H\}$ NMR spectra show a singlet (at δ 14.7 for **2a**; at δ –16.9 for **2b**; at δ 33.5 for **2c**), while a high-field doublet assigned to the bridging hydride is seen in the ^{1}H NMR spectra. The $J_{P–H}$ coupling constants (*ca.* 6-10 Hz) associated with the doublets are relatively small suggesting that the hydride lies *cis* to the phosphine which is also observed in the solid-state.

For the bis(phosphine) derivatives **3a-c**, only **3a** has been characterized crystallographically while the other two have been characterized by spectroscopic means only. Fig. 5 shows the solid-state molecular structure of **3a** with the caption containing selected bond lengths and angles. The cluster core consists of an osmium triangle with three distinctly different osmium-osmium bond lengths ranging from 2.78865(18) to 3.06618(18) Å. Interestingly, the sac and hydride bridge separate osmium-osmium edges in **3a**. While the sac ligand bridges the shortest osmium-osmium edge [Os(1)–Os(2) 2.78865(18) Å], the longest edge [Os(1)–Os(3) 3.06618(18) Å] is spanned by the hydride. Akin to the mono-(phosphine) derivatives one of the PPh_3 ligands occupies an equatorial site on the osmium directly bonded to carbonylic oxygen, whilst the other coordinates to the remote osmium occupying an equatorial site on it. There is however a subtle difference between mono- and bis-(phosphine) substituted clusters **2a** and **3a** with respect to the equatorial coordination site occupied by

PPh_3 on oxygen-bound osmium. In **3a**, this phosphine lies *trans* to the saccharinate-bridged osmium-osmium vector whereas in the mono-substituted derivatives (**2a-c**) it always adopts a *cis*-configuration with respect to this osmium-osmium vector (Scheme 4). In **3a**, the phosphine ligands are spatially orientated in such a way that they adopt a *cis*-configuration with respect to the Os(1)–Os(3) vector and this *cis*-configuration of phosphines is most probably responsible for the elongation of Os(1)–Os(3) edge compared to other edges. The Os–N [2.140(2) Å], Os–O [2.170(2) Å] and Os–P [2.3881(8) and 2.3756(8) Å] bond distances are almost identical within the experimental error to those observed in **2a**.

NMR data for **3a** suggest that it exists in two isomeric forms in solution. The $^{31}P\{^1H\}$ NMR spectrum displays four singlets at δ 12.5, 10.4, –3.0, –4.6 with an intensity ratio of 2:1:1:2. The hydride region of the ^1H NMR spectrum shows a doublet at δ –10.25 (d, J 10 Hz) for the major isomer and a triplet at δ –11.87 (t, J 7.5 Hz) for the minor isomer in 2:1 intensity ratio, similar to the intensity ratio observed for the major and minor isomers in the $^{31}P\{^1H\}$ NMR spectrum. In the solid-state, the hydride lies *cis* to both PPh_3 ligands for which we would expect a doublet of doublets (or triplet) in the ^1H NMR spectrum. Thus, we assume that the solid-state structure is that of the minor isomer in solution (**3a**$_1$ in Chart 2). For the major isomer, we observe a doublet ($J_{P–H}$ 10 Hz) similar to that observed for mono-(phosphine) substituted **2a**. We thus assume that the major isomer in solution is most probably **3a**$_2$ (Chart 2) since the PPh_3 ligand occupies this equatorial coordination site in **2a**. Similar fluxional behaviour, involving migration of hydride along different osmium-osmium edges and/or movement of phosphines between two equatorial sites on the same osmium, has been observed in related triosmium clusters such as $Os_3(CO)_9(PR_3)(\mu\text{-}H)(\mu\text{-}CH_3CH_2C{=}NCH_2CH_2CH_3)$ (R = Ph, OEt) [26]. The aromatic region of the ^1H NMR spectrum is uninformative showing resonance for phenyl and sac ring protons of both isomers.

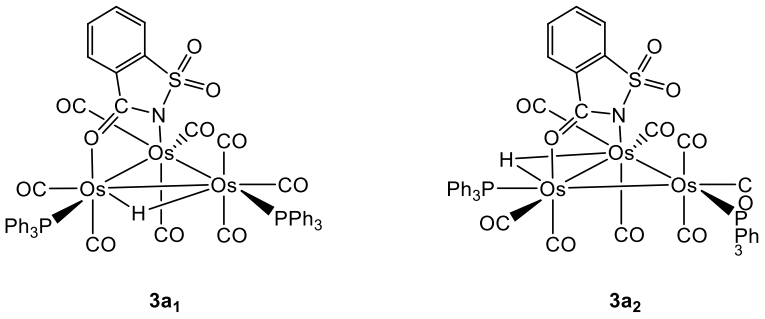

Chart 2. Proposed isomers of **3a**

Clusters **3b** and **3c** also show two isomeric forms in solution. In the $^{31}P\{^{1}H\}$ NMR spectrum of **3b**, the major isomer appears as two singlets at δ –18.8 and –31.4, while the minor isomer shows another set of singlets at δ –18.3 and –42.3. The hydride region of its ^{1}H NMR spectrum displays a doublet of doublets at δ –9.87 (dd, J 12.5, 10 Hz) for the major isomer and a triplet at δ –11.64 (t, J 10 Hz) attributed to the minor isomer. Again we assume that the minor isomer (**3b$_1$** in Chart 3) has the same structure as **3a$_1$**, whereas the coupling constants associated with the doublet of doublets suggest that one PTh_3 ligand lies *cis* to the hydride while the other lies *trans* to it as shown in **3b$_2$** and **3b$_3$** (Chart 3). The major isomer is most probably **3b$_2$** since the phosphine on oxygen-bound osmium lies *cis* to the saccharinate-bridged osmium-osmium vector in it which is observed in the mono-(phosphine) substituted derivatives.

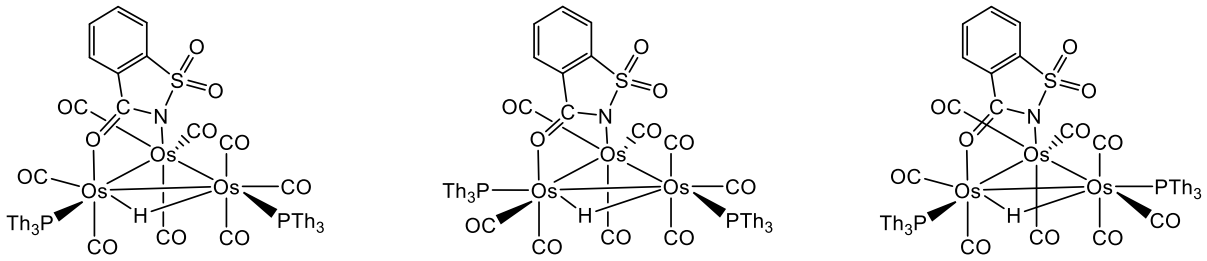

Chart 3. Possible isomers of **3b**

The hydride region of the ^{1}H NMR spectrum of **3c** shows two doublet of doublets at δ –10.17 (dd, J 15, 10 Hz) and –11.06 (dd, J 40, 20 Hz) with an intensity ratio of *ca.* 7:1. Likewise its $^{31}P\ \{^{1}H\}$ NMR spectrum displays two sets of singlets: at δ –31.6 and –49.2 for the major isomer and at δ –34.7 and –47.6 for the minor isomer. Considering the probable isomers proposed for bis-(phosphine) substituted **3a** and **3b**, and the $J_{P–H}$ coupling constant associated with the hydride resonances observed in the ^{1}H NMR spectrum of **3c**, we suggests that the latter may adopt any two isomeric forms in solution among the three probable isomers proposed for **3b** in Chart 3.

3. Conclusions

The saccharinate-bridged triosmium cluster $Os_3(CO)_{10}(\mu\text{-}H)(\mu\text{-}sac)$ (**1**) has been prepared from the reactions of lightly stabilized $Os_3(CO)_{10-n}(NCMe)_n$ (n = 1, 2) with saccharin at moderate temperatures. Cluster **1** is formed by the oxidative-addition of N–H bond of saccharin at the cluster surface followed by coordination of the carbonylic oxygen to an adjacent osmium. The triosmium core is retained in **1** and it contains only one sac ligand, whereas multiple addition of sac ligand as well as cluster fragmentation have been observed in similar reactions between $Ru_3(CO)_{12}$ and saccharin. The reactivity of this cluster towards various monodentate phosphines has also been studied. Cluster **1** undergoes stepwise carbonyl substitution when treated with PR_3 (R = Ph, Th, Fu) in boiling toluene and forms mono- and bis-(phosphine) substituted derivatives $Os_3(CO)_9(PR_3)(\mu\text{-}H)(\mu\text{-}sac)$ (**2**) and $Os_3(CO)_8(PR_3)_2(\mu\text{-}H)(\mu\text{-}sac)$ (**3**), respectively. In the mono-substituted derivatives, the phosphine occupies an equatorial position on the osmium directly bonded to carbonylic oxygen. The second phosphine occupies another equatorial position on the remote osmium in the bis-(phosphine) substituted derivatives. The mono-substituted derivatives retain their solid-state structure in solution, whereas the bis-(phosphine) substituted derivatives exists in two isomeric forms in solution due to either migration of hydride along different osmium-osmium edges and/or movement of phosphines between two equatorial sites on the same osmium. Studies on the reactivity of **1** towards other substrates are ongoing in our laboratory and will be reported elsewhere.

4. Experimental Section

4.1. General

All reactions were carried out under a dry nitrogen atmosphere using standard Schlenk techniques unless otherwise stated. Reagent grade solvents were dried using appropriate drying agents and distilled prior to use by standard methods. $Os_3(CO)_{12}$ was purchased from Strem Chemical Inc. and used without further purification. Saccharin and phosphines were purchased from Across Chemicals Inc. and used as received and $Os_3(CO)_{10}(NCMe)_2$ was prepared according to published methods [27]. Products were separated in the air by TLC plates coated with 0.25mm of silica gel (HF_{254}-type 60, E. Merck, Germany). Infrared spectra were recorded on a Shimadzu FTIR Prestige 21 spectrophotometer and the NMR spectra were recorded on a Varian Unity plus 500 spectrometer. All chemical shifts are reported in δ units and are referenced to the residual protons of the deuterated solvents (^1H) and to external

H_3PO_4 (^{31}P). Elemental analyses were performed by the Microanalytical laboratory of Wazed Miah Science Research Centre at Jahangirnagar University.

4.2. Reaction of $Os_3(CO)_{11}(NCMe)$ with saccharin

Saccharin (44 mg, 0.240 mmol) was added to a benzene solution (20 mL) of $Os_3(CO)_{11}(NCMe)_2$ (110 mg, 0.120 mmol) and the reaction mixture was heated to reflux for 5 h. The colour of the reaction mixture changed from yellow to orange by this time and the consumption of $Os_3(CO)_{11}(NCMe)$ was monitored by analytical TLC. The reaction mixture was then allowed to cool at room temperature. The solvent was removed under vacuum and the residue separated by TLC on silica gel. Elution with hexane/CH_2Cl_2 (v/v 7:3) developed a yellow band which afforded $Os_3(CO)_{10}(\mu\text{-H})(\mu\text{-sac})$ (**1**) (42 mg, 34%) after recrystallization from hexane/CH_2Cl_2 at 4 °C. A similar reaction between $Os_3(CO)_{11}(NCMe)$ and saccharin at room temperature in CH_2Cl_2 for 3 d gave **1** in 15% yield after chromatographic separation and work up described above. Data for **1**: Anal. Calcd for $C_{17}H_5N_1O_{13}Os_3S_1$: C, 19.75; H, 0.49; N, 1.35. Found: C, 20.17; H, 0.55; N, 1.39%. IR (νCO, M–CO, CH_2Cl_2): 2115m, 2078s, 2066s, 2029s, 2017s, 1986m cm^{-1}. IR (νCO, sac, KBr): 1672 cm^{-1}. ^1H NMR ($CDCl_3$): δ 7.82 (s,br, 1H), 7.59 (s,br, 3H), –11.61 (s, 1H).

4.3. Reaction of $Os_3(CO)_{10}(NCMe)_2$ with saccharin

A benzene solution (20 mL) of $Os_3(CO)_{10}(NCMe)_2$ (130 mg, 0.139 mmol) and saccharin (306 mg, 1.67 mmol) was heated to reflux for 2 h. The colour of the reaction mixture changed from yellow to orange by this time and the consumption of $Os_3(CO)_{10}(NCMe)_2$ was monitored by analytical TLC. The reaction mixture was then allowed to cool at room temperature. The solvent was removed under reduced pressure and the residue separated by TLC on silica gel. Elution with hexane/CH_2Cl_2 (v/v 7:3) developed a yellow band which afforded $Os_3(CO)_{10}(\mu\text{-H})(\mu\text{-sac})$ (**1**) (88 mg, 61%) after recrystallization from hexane/CH_2Cl_2 at 4 °C. A similar reaction between $Os_3(CO)_{10}(NCMe)_2$ and saccharin at room temperature in CH_2Cl_2 for 48 h gave **1** in 20% yield after chromatographic separation and work up described above.

*4.4. Reaction of $Os_3(CO)_{10}(\mu\text{-H})(\mu\text{-sac})$ (**1**) with PPh_3*

To a toluene solution (20 mL) of **1** (32 mg, 0.031 mmol) was added PPh_3 (17 mg, 0.065 mmol) and the reaction mixture was then heated to reflux for 5 h. The reaction mixture was allowed to cool at room temperature. The solvent was removed under vacuum and the residue chromatographed by TLC on silica gel. Elution with hexane/CH_2Cl_2 (v/v 7:3) developed a two bands which afforded $Os_3(CO)_9(PPh_3)(\mu\text{-}H)(\mu\text{-sac})$ (**2a**) (22 mg, 56%) and $Os_3(CO)_8(PPh_3)_2(\mu\text{-}H)(\mu\text{-sac})$ (**3a**) (13 mg, 28%) in order of elution after recrystallization from hexane/CH_2Cl_2 at 4 °C. Data for **2a**: Anal. Calcd for $C_{34}H_{20}N_1O_{12}Os_3P_1S_1$: C, 32.20; H, 1.59; N, 1.10. Found: C, 32.77; H, 1.68; N, 1.13%. IR (νCO, CH_2Cl_2): 2098s, 2059s, 2021vs, 2002s, 1971m, 1945w cm^{-1}. ^1H NMR ($CDCl_3$): δ 7.69 (m, 1H), 7.50 (m, 7H), 7.36 (m, 10H), 7.01 (m, 1H), –11.11 (d, J 10 Hz, 1H). $^{31}P\{^1H\}$ NMR ($CDCl_3$): δ 14.7 (s). Data for **3a**: Anal. Calcd for $C_{51}H_{35}N_1O_{11}Os_3P_2S_1$: C, 40.77; H, 2.35; N, 0.93. Found: C, 40.44; H, 2.36; N, 0.97%. IR (νCO, CH_2Cl_2): 2098w, 2078m, 2038s, 2005vs, 1993s, 1954m cm^{-1}. ^1H NMR ($CDCl_3$): aromatic region: major isome: δ 7.72 (d, J 7.5 Hz, 1H), 7.54 (m, 2H), 7.46 (m, 3H), 7.34 (m, 15H), 7.20 (m, 12H), 6.43 (d, J 7.5 Hz, 1H); hydride region: major isomer: δ –10.25 (d, J 10 Hz); minor isomer: δ –11.87 (t, J 7.5 Hz). $^{31}P\{^1H\}$ NMR ($CDCl_3$): major isomer: δ 12.5 (s), –4.6 (s); minor isomer: δ 10.4 (s), –3.0 (s). Major isomer : minor isomer = 2:1.

*4.5. Reaction of $Os_3(CO)_{10}(\mu\text{-}H)(\mu\text{-sac})$ (**1**) with PTh_3*

$P(C_4H_3S)_3$ (23 mg, 0.082 mmol) was added to a toluene solution (20 mL) of **1** (42 mg, 0.041 mmol) and the reaction mixture was then heated to reflux for 4 h. The reaction mixture was allowed to cool at room temperature. The solvent was removed under vacuum and the residue subjected to TLC on silica gel. Elution with hexane/CH_2Cl_2 (v/v 7:3) developed a two bands which afforded $Os_3(CO)_9(PTh_3)(\mu\text{-}H)(\mu\text{-sac})$ (**2b**) (27 mg, 51%) and $Os_3(CO)_8(PTh_3)_2(\mu\text{-}H)(\mu\text{-sac})$ (**3b**) (18 mg, 29%) in order of elution after recrystallization from hexane/CH_2Cl_2 at 4 °C. Data for **2b**: Anal. Calcd for $C_{28}H_{14}N_1O_{12}Os_3P_1S_4$: C, 25.94; H, 1.87; N, 1.08. Found: C, 26.38; H, 1.91; N, 1.04%. IR (νCO, CH_2Cl_2): 2099s, 2061s, 2022vs, 2005s, 1973m, 1951w cm^{-1}. ^1H NMR ($CDCl_3$): δ 7.72 (d, J 7.5 Hz, 1H), 7.60 (m, 3H), 7.55 (t, J 7.5 Hz, 1H), 7.49 (m, 4H), 7.16 (d, J 7.5 Hz, 1H), 7.12 (m, 3H), –11.16 (d, J 6 Hz, 1H). $^{31}P\{^1H\}$ NMR ($CDCl_3$): δ –16.9 (s). Data for **3b**: Anal. Calcd for $C_{39}H_{23}N_1O_{11}Os_3P_2S_7$: C, 30.44; H, 1.51; N, 0.91. Found: C, 30.93; H, 1.56; N, 0.98%. IR (νCO, CH_2Cl_2): 2099w, 2078s, 2020s, 2011s, 1992m, 1967w cm^{-1}. ^1H NMR ($CDCl_3$): aromatic region: major isomer: δ 7.74 (m, 1H), 7.57-7.30 (m, 14H), 7.08 (m, 2H), 7.03 (m, 3H), 6.89 (m, 2H); hydride region: major isomer: δ –9.87 (dd, J 12.5, 10 Hz); minor isomer: δ –11.64 (t, J 10 Hz). $^{31}P\{^1H\}$ NMR ($CDCl_3$): major

isomer: δ –18.8 (s), –31.4 (s); minor isomer: δ –18.3 (s), –42.3 (s). Major:minor isomer *ca.* 2:1.

*4.6. Reaction of $Os_3(CO)_{10}(\mu$-H)(μ-sac) (**1**) with PFu_3*

A toluene solution (20 mL) of **1** (40 mg, 0.039 mmol) and $P(C_4H_3O)_3$ (18 mg, 0.078 mmol) was heated to reflux for 5 h. The reaction mixture was allowed to cool at room temperature. The solvent was removed under reduced vacuum and the residue separated by TLC on silica gel. Elution with hexane/CH_2Cl_2 (v/v 7:3) developed a two bands which afforded $Os_3(CO)_9(PFu_3)(\mu$-H)(μ-sac) (**2c**) (19 mg, 40%) and $Os_3(CO)_8(PFu_3)_2(\mu$-H)(μ-sac) (**3c**) (9 mg, 16%) in order of elution after recrystallization from hexane/CH_2Cl_2 at 4 °C. Data for **2c**: Anal. Calcd for $C_{28}H_{14}N_1O_{15}Os_3P_1S_1$: C, 27.16; H, 1.14; N, 1.13. Found: C, 27.67; H, 1.21; N, 1.19%. IR (νCO, CH_2Cl_2): 2099s, 2062s, 2024vs, 2006s, 1973m, 1957w cm^{-1}. ^1H NMR ($CDCl_3$): δ 7.75 (d, J 7.5 Hz, 1H), 7.66 (m, 3H), 7.57 (t, J 7.5 Hz, 1H), 7.49 (t, J 7.5 Hz, 1H), 7.13 (d, J 7.5 Hz, 1H), 6.82 (m, 3H), 6.46 (m, 3H), –11.39 (d, J 6 Hz, 1H). $^{31}P\{^1H\}$ NMR ($CDCl_3$): δ 33.5 (s). Data for **3c**: Anal. Calcd for $C_{39}H_{23}N_1O_{17}Os_3P_2S_1$: C, 32.48; H, 1.61; N, 0.97. Found: C, 32.48; H, 1.70; N, 1.02%. IR (νCO, CH_2Cl_2): 2099w, 2079s, 2023s, 2016s, 2003s, 1992sh, 1967m cm^{-1}. ^1H NMR ($CDCl_3$): δ aromatic region: both isomers: δ 7.77-6.37 (m, 22H); hydride region: major isomer: δ –10.17 (dd, J 15, 10 Hz); minor isomer: δ –11.06 (dd, J 40, 20 Hz). $^{31}P\{^1H\}$ NMR ($CDCl_3$): δ major isomer: δ –31.6 (s), –49.2 (s); minor isomer: δ –34.7 (s), –47.6 (s). Major:minor isomer *ca.* 7:1.

.

4.7. Crystal structure determinations

Single crystals suitable for X-ray diffraction analysis were grown by slow diffusion of hexane into a CH_2Cl_2 solution of **1**, **2a-c** and **3a**. The crystals were mounted on a SuperNova, Dual, Cu at zero, Atlas diffractometer using a Nylon Loop. The crystals were kept at 150(1) K during data collection. Using Olex2 [28], the structure was solved with the ShelXS [29] structure solution program using Direct Methods for **1** and **2a**, while using Patterson Method for **2b**. The structure of **3a** was solved with the olex2.solve [30] structure solution program using Charge Flipping and the structure of **2c** was solved with the Superflip [31] structure solution program using Charge Flipping. The structures were refined with the ShelXL [32] refinement package using Least Squares minimisation. In cluster **2b**, two of the thienyl rings were disordered. These were modelled as if the planes of the thienyl rings were rotated 180

degrees to generate a common set of positions for pairs of S/C atoms. The atomic displacement parameters were set equal and the occupancies refined. In the converged model the two positions for one thienyl had a 73:28 distribution while in the second thienyl the distribution was 70:30. All non-hydrogen atoms were refined anisotropically and hydrogen atoms (except those directly bonded to metals) were included using a riding model. The details of the data collection and structure refinement are given in Table 2.

Appendix A. Supplementary material

CCDC 1411308 (for **1**), 1411309 (for **2a**), 1411310 (for **3a**), 1411311 (for **2b**) and 1411312 (for **2c**) contain the supplementary crystallographic data for this paper. These data can be obtained free of charge from The Cambridge Crystallographic Data Centre via www.ccdc.cam.ac.uk/data_request/cif.

Acknowledgements

We thank the Ministry of Education, the Government of the People's Republic of Bangladesh for financial support.

References

[1] L.O. Nabors, C.G. Robert, Alternative Sweeteners, 2nd ed., Marcel Dekker, New York, 1991.
[2] E.J. Baran, V.Y. Yilmaz, Coord. Chem. Rev. 250 (2006) 1980-1999.
[3] E.J. Baran, Quím. Nova 28 (2005) 326-328.
[4] S. Buck, G. Maas, J. Organomet. Chem. 691 (2006) 2774-2784.
[5] M. Grohmann, G. Maas, Tetrahedron 63 (2007) 12172-12178.
[6] M. Grohmann, S. Buck, L. Schäffler, G. Maas, Adv. Synth. Catal. 348 (2006) 2203-2211.
[7] T.-T. Thai, B. Therrien, G. Süss-Fink, J. Organomet. Chem. 696 (2011) 3285-3291.
[8] E.-J. Schier, W. Sacher, W. Beck, Z. Naturforsch. 42b (1987) 1424-1434.
[9] B.F.G. Johnson, J. Lewis, T.I. Odiaka, P. R. Raithby, J. Organomet. Chem. 216 (1981) C56-C60.

[10] L.R. Falvello, J. Gomez, I. Pascual, M. Tomás, E.P. Urriolabeitia, A.J. Schultz, Inorg. Chem. 40 (2001) 4455–4463.
[11] P. Naumov, G. Jovanovski, S.-Z. Hu, I.-H. Suh, I.A. Razak, S. Chantrapromma, H.-K. Fun, S.W. Ng, Acta Crystallogr., Sect. C 57 (2001) 1016-1019.
[12] M.D. Santana, R.García-Bueno, G. García, G. Sánchez, J. García, A.R. Kapdi, M. Naik, S. Pednekar, J. Pérez, L. García, E. Pérezd, J.L. Serrano, Dalton Trans. 41 (2012) 3832-3842.
[13] (a) F.A. Cotton, L.R. Falvello, W. Schwotzer, C.A. Murillo, G. Valle-Bourrouet, Inorg. Chim. Acta 190 (1991) 89-96.
(b) N.M. Alfaro, F.A. Cotton, L.M. Daniels, C.A. Murillo, Inorg. Chem. 31 (1992) 2718-2723.
[14] L. D'Ornelas, T. Castrillo, L. Hernández de B., A. Narayan, R. Atencio, Inorg. Chim. Acta 342 (2003) 1-8.
[15] (a) J.A. Cabeza, Eur. J. Inorg. Chem. (2002) 1559-1570 and references therein; (b) J.A. Cabeza, I. del Río, S. García-Granda, V. Riera, M. Suárez, Organometallics 21 (2002) 2540-2543.
[16] (a) S.E. Kabir, D.S. Kolwaite, E. Rosenberg, L.G. Scott, T. McPhillips, R. Duque, M. Day, K.I. Hardcastle, Organometallics 15 (1996) 1979-1988; (b) E. Rosenberg, S.E. Kabir, K.I. Hardcastle, M. Day, E. Wolf, Organometallics 9 (1990) 2214-2217; (c) S.E. Kabir, M. Day, M. Irving, T. McPhilllps, H. Minassian, E. Rosenberg, K.I. Hardcastle, Organometallics 10 (1991) 3997-4004. (d) M. Day, D. Espitia, K.I. Hardcastle, S.E. Kabir, T. MePhillips, E. Rosenberg, Organometallics 12 (1993) 2309-2324.
[17] (a) P.M. Lausarot, G.A. Vaglio, M. Valle, A. Tiripicchio, M.T. Camellini, P. Gariboldi, J. Organomet. Chem. 291 (1985) 221-229; (b) G.R. Frauenhoff, S.R. Wilson, J.R. Shapley, Inorg. Chem. 30 (1991) 78-85.
[18] Y. Okaya, Acta Crystallogr. B25 (1969) 2257-2263.
[19] (a) A. Rahaman, F.R. Alam, S. Ghosh, M. Haukka, S.E. Kabir, E. Nordlander, G. Hogarth, J. Organomet. Chem. 730 (2013) 123-131; (b) M.K. Hossain, S. Rajbangshi, A. Rahaman, M.A.H. Chowdhury, T.A. Siddiquee, S. Ghosh, M.G. Richmond, E. Nordlander, G. Hogarth, S.E. Kabir, J. Organomet. Chem. 760 (2014) 231-239.; (c) M.A. Rahman, N. Begum, S. Ghosh, M.K. Hossain, G. Hogarth, D.A. Tocher, E. Nordlander, S.E. Kabir, J. Organomet. Chem. 696 (2011) 607-612; (d) S. Ghosh, A.K. Das, N. Begum, D.T. Haworth, S.V. Lindeman, J.F. Gardinier, T.A. Siddiquee, D.W. Bennett, E. Nordlander, G. Hogarth, S.E. Kabir, Inorg. Chim. Acta 362 (2009) 5175-5182; (e) M.N. Uddin, N. Begum, M.R.

Hassan, G. Hogarth, S.E. Kabir, M.A. Miah, E. Nordlander, D.A. Tocher, J. Chem. Soc., Dalton Trans. (2008) 6219-6230.

[20] (a) A. Rahaman, F.R. Alam, M.K. Hossain, A.F. Abdel-Magied, S. Ghosh, D.A. Tocher, M. Haukka, S.E. Kabir, E. Nordlander, G. Hogarth, Inorg. Chim. Acta 430 (2015) 208-215; (b) A. Rahaman, F.R. Alam, S. Ghosh, D.A. Tocher, M. Haukka, S.E. Kabir, E. Nordlander, G. Hogarth, J. Organomet. Chem. 751 (2014) 326–335.

[21] (a) A.K. Raha, M.N. Uddin, S. Ghosh, A.R. Miah, M.G. Richmond, D.A. Tocher, E. Nordlander, G. Hogarth, S.E. Kabir, J. Organomet. Chem. 751 (2014) 399-411; (b) S. Rana, S. Ghosh, S.E. Kabir, J. Bangladesh Chem. Soc. 25 (2012) 1-6; (c) M.I. Hossain, M.D.H. Sikder, S. Ghosh, S.E. Kabir, G. Hogarth, L. Salassa, Organometallics 31 (2012) 2546-2558; (d) S. Karmaker, S. Ghosh, S.E. Kabir, D. T. Haworth, S. V. Lindeman, Inorg. Chim. Acta 382 (2012) 199-202.

[22] (a) S. Ghosh, G. Hogarth, D.A. Tocher, E. Nordlander, S.E. Kabir, Inorg. Chim. Acta 363 (2010) 1611-1614; (b) M.N. Uddin, M.A. Mottalib, N. Begum, S. Ghosh, A.K. Raha, D.T. Haworth, S.V. Lindeman, T.A. Siddiquee, D.W. Bennett, G. Hogarth, E. Nordlander, S.E. Kabir, Organometallics 28 (2009) 1514-1523; (c) S. Ghosh, M. Khatun, D.T. Haworth, S.V. Lindeman, T.A. Siddiquee, D.W. Bennett, G. Hogarth, E. Nordlander, S.E. Kabir, J. Organomet. Chem. 694 (2009) 2941-2948; (d) S. Ghosh, S. Rana, D.A. Tocher, G. Hogarth, E. Nordlander, S.E. Kabir, J. Organomet. Chem. 694 (2009) 3312-3319;

[23] M. Ackermann, A. Pascariu, T. Höcher, H.-U. Siehl, S. Berger, J. Am. Chem. Soc. 128 (2006) 8434-8440.

[24] (a) N.G. Anderson, B.A. Keay, Chem. Rev. 101 (2001) 997-1030; (b) M. Sakai, H. Hayashi, N. Miyaura, Organometallics 16 (1997) 4229-4231; (c) E. Shirakawa, K. Yamasaki, T. Hiyama, Synthesis (1998) 1544-1549; (d) B.M. Trost, Y.H. Rhee, J. Am. Chem. Soc. 121 (1999) 11680-11683.

[25] (a) J.C. Anderson, H. Namli, C.A. Roberts, Tetrahedron 53 (1997) 15123-15134; (b) W.A. Herrmann, S. Brossmer, K. Öfele, M. Beller, H. Fischer, J. Mol. Catal. A: Chem. 103 (1995) 133-146; (c) V. Farina, S.R. Baker, D.A. Benigni, C. Sapino, Tetrahedron Lett. 29 (1988) 5739-5742.

[26] M. Day, D. Espitia, K.I. Hardcastle, S.E. Kabir, E. Rosenberg, R. Gobetto, L. Milone, D. Osella, Organometallics 10 (1991) 3550-3559.

[27] B. F. G. Johnson, J. Lewis and D. A. Pippard, *J. Chem. Soc., Dalton Trans.*, 1981, 407-412.

[28] O.V. Dolomanov, L.J. Bourhis, R.J. Gildea, J.A.K. Howard, H. Puschmann, J. Appl. Cryst. 42 (2009) 339-341.
[29] G.M. Sheldrick, Acta Cryst. A64 (2008) 112-122.
[30] L.J. Bourhis, O.V. Dolomanov, R.J. Gildea, J.A.K. Howard, H.Puschmann, (2013) in preparation.
[31] (a) L. Palatinus, G. Chapuis, J. Appl. Cryst. 40 (2007) 786-790; (b) L. Palatinus, A. van der Lee, J. Appl. Cryst. 41 (2008) 975-984; (c) L. Palatinus, S.J. Prathapa, S. van Smaalen, J. Appl. Cryst. 45 (2012) 575-580.
[32] G.M. Sheldrick, Acta Cryst. A64 (2008) 112-122.

Table 1. Selected bond lengths of **1** and **2a**-**c**

Compound	**1**	**2a**	**2b**	**2c**[a]
Os–Os[b]	2.9224(3), 2.8934(3), 2.8730(3)	2.9530(2), 2.8989(3), 2.8982(3)	2.9541(3), 2.8803(3), 2.8734(3)	2.9567(3), 2.8755(3), 2.8670(3)
Os–O	2.134(4)	2.158(3)	2.154(4)	2.154(4)
Os–N	2.149(4)	2.153(4)	2.143(5)	2.158(4)
Os–P	–	2.3704(12)	2.3428(16)	2.3419(14)

[a] Bond distances are reported for one molecule; [b] All bond distances are reported in Å

Table 2. Crystallographic and structural refinement data for triosmium sac complexes

Compound	**1**	**2a**	**3a**	**2b**	**2c**
Empirical formula	$C_{17}H_5NO_{13}Os_3S$	$C_{34}H_{20}NO_{12}Os_3PS$	$C_{51}H_{35}NO_{11}Os_3P_2S \cdot CH_2Cl_2$	$C_{28}H_{13}NO_{12}Os_3PS_4$	$C_{28}H_{14}NO_{15}Os_3PS$
Formula weight	1033.88	1268.14	1587.32	1285.20	1238.03
Temperature (K)	150(1)	150(1)	149.96(10)	150.00(10)	150(1)
Wavelength (Å)	0.71073	0.71073	0.71073	0.71073	0.71073
Crystal system	orthorhombic	monoclinic	triclinic	monoclinic	triclinic
Space group	*Pbca*	$P2_1/c$	*P*-1	$P2_1/n$	*P*-1
Unit cell dimensions					
a (Å)	8.80680(9)	14.7493(2)	11.4048(3)	9.3066(2)	9.1388(2)
b (Å)	15.5256(2)	12.9835(1)	13.7827(3)	30.7042(6)	19.2162(4)
c (Å)	33.4463(4)	19.2378(2)	18.5882(5)	12.2099(3)	20.4044(5)
α (°)	90	90	75.851(2)	90	104.326(2)
β (°)	90	101.8832(10)	72.723(2)	99.646(2)	91.231(2)
γ (°)	90	90	68.531(2)	90	94.598(1)
Volume (Å^3)	4573.14(9)	3605.05(7)	2566.0(1)	3439.7(1)	3457.5(1)
Z	8	4	2	4	4
Density (calculated) (Mg/m^3)	3.003	2.336	2.054	2.482	2.378
Absorption coefficient (mm^{-1})	16.789	10.713	7.678	11.405	11.173
F(000)	3696.0	2344.0	1504.0	2364.0	2272.0
Crystal size (mm^3)	0.26 × 0.12 × 0.08	0.28 × 0.26 × 0.22	0.28 × 0.08 × 0.04	0.3 × 0.1 × 0.08	0.3 × 0.08 × 0.06
2θ range for data collection (°)	5.786 to 55.812	5.614 to 55.742	5.824 to 58.934	5.76 to 58.802	5.956 to 55.608
Index ranges	$-11 \le h \ge 11$	$-18 \le h \ge 19$	$-15 \le h \ge 14$	$-12 \le h \ge 11$	$-11 \le h \ge 11$
	$-20 \le k \ge 19$	$-26 \le k \ge 16$	$-17 \le k \ge 17$	$-40 \le k \ge 39$	$-25 \le k \ge 25$
	$-43 \le l \ge 43$	$-24 \le l \ge 24$	$-24 \le l \ge 25$	$-16 \le l \ge 16$	$-26 \le l \ge 26$
Reflections collected	56091	44655	40609	55280	44084
Independent reflections	5335 [R_{int} = 0.0529]	8226 [R_{int} = 0.0667]	12598 [R_{int} = 0.0352]	8802 [R_{int} = 0.0792]	15333 [R_{int} = 0.0299]
Data/restraints/parameters	5335 / 0 / 321	8226 / 0 / 474	12598 / 0 / 653	8802 / 0 / 444	15333 / 0 / 851
Goodness-of-fit on F^2	1.182	1.085	1.037	1.015	1.022
Final *R* indices [$I>2\sigma(I)$]	R_1 = 0.0258,	R_1 = 0.0290,	R_1 = 0.0239,	R_1 = 0.0394,	R_1 = 0.0279,
	wR_2 = 0.0529	wR_2 = 0.0626	wR_2 = 0.0442	wR_2 = 0.0872	wR_2 = 0.0607
R indices (all data)	R_1 = 0.0276,	R_1 = 0.0333,	R_1 = 0.0298,	R_1 = 0.0464,	R_1 = 0.0340,
	wR_2 = 0.0535	wR_2 = 0.0653	wR_2 = 0.0465	wR_2 = 0.0921	wR_2 = 0.0637
Largest diff. peak and hole (eÅ^{-3})	1.55 and –1.27	1.73 and –2.88	0.94 and –0.90	3.89 and –2.58	3.41 and –1.28

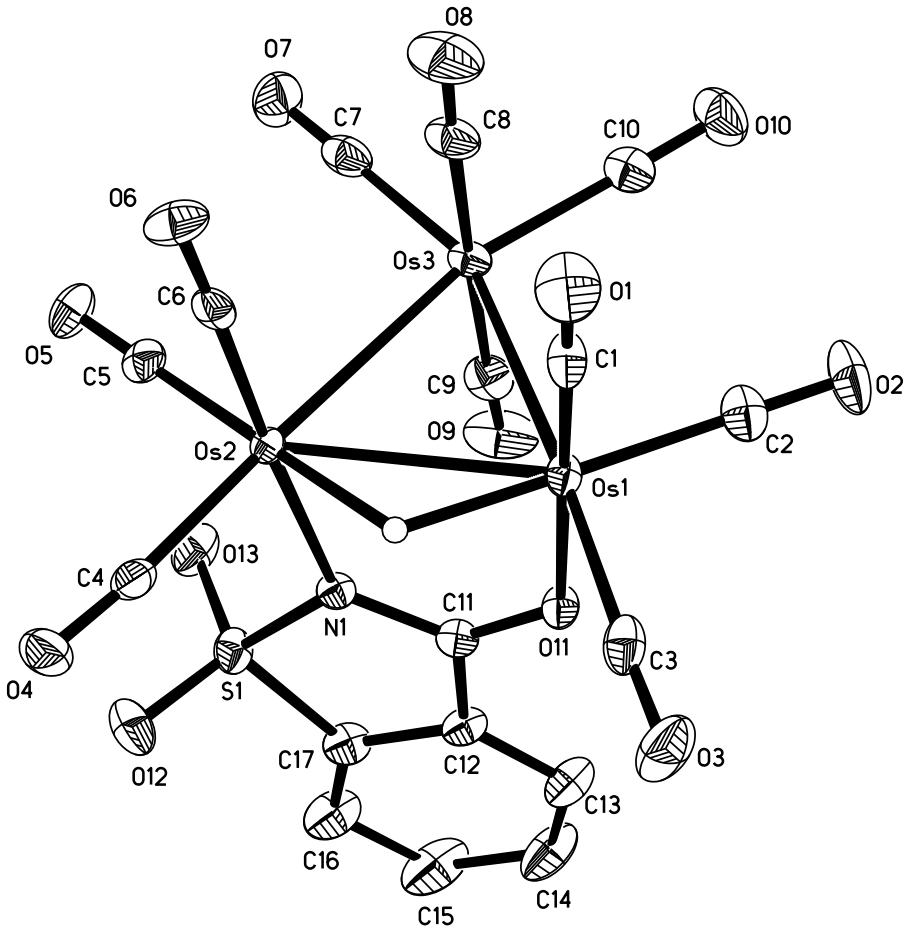

Fig. 1. The solid-state molecular structure of $Os_3(CO)_{10}(\mu\text{-H})(\mu\text{-sac})$ (**1**), showing 50% probability thermal ellipsoids. Ring hydrogen atoms were omitted for clarity. Selected interatomic distances (Å) and angles (°): Os(1)–Os(2) 2.9224(3), Os(1)–Os(3) 2.8730(3), Os(2)–Os(3) 2.8934(3), Os(1)–O(11) 2.134(4), Os(2)–N(1) 2.149(4), Os(2)–Os(1)–Os(3) 59.895(7), Os(1)–Os(2)–Os(3) 59.206(7), Os(1)–Os(3)–Os(2) 60.899(7), O(11)–Os(1)–Os(2) 83.89(10), O(11)–Os(1)–Os(3) 90.00(10), O(11)–Os(1)–C(2) 88.75(19), O(11)–Os(1)–C(3) 85.4(2), O(11)–Os(1)–C(1) 175.2(2), N(1)–Os(2)–Os(1) 79.25(12), N(1)–Os(2)–Os(3) 90.05(12), N(1)–Os(2)–C(4) 90.8(2), N(1)–Os(2)–C(5) 95.2(2), N(1)–Os(2)–C(6) 175.5(2).

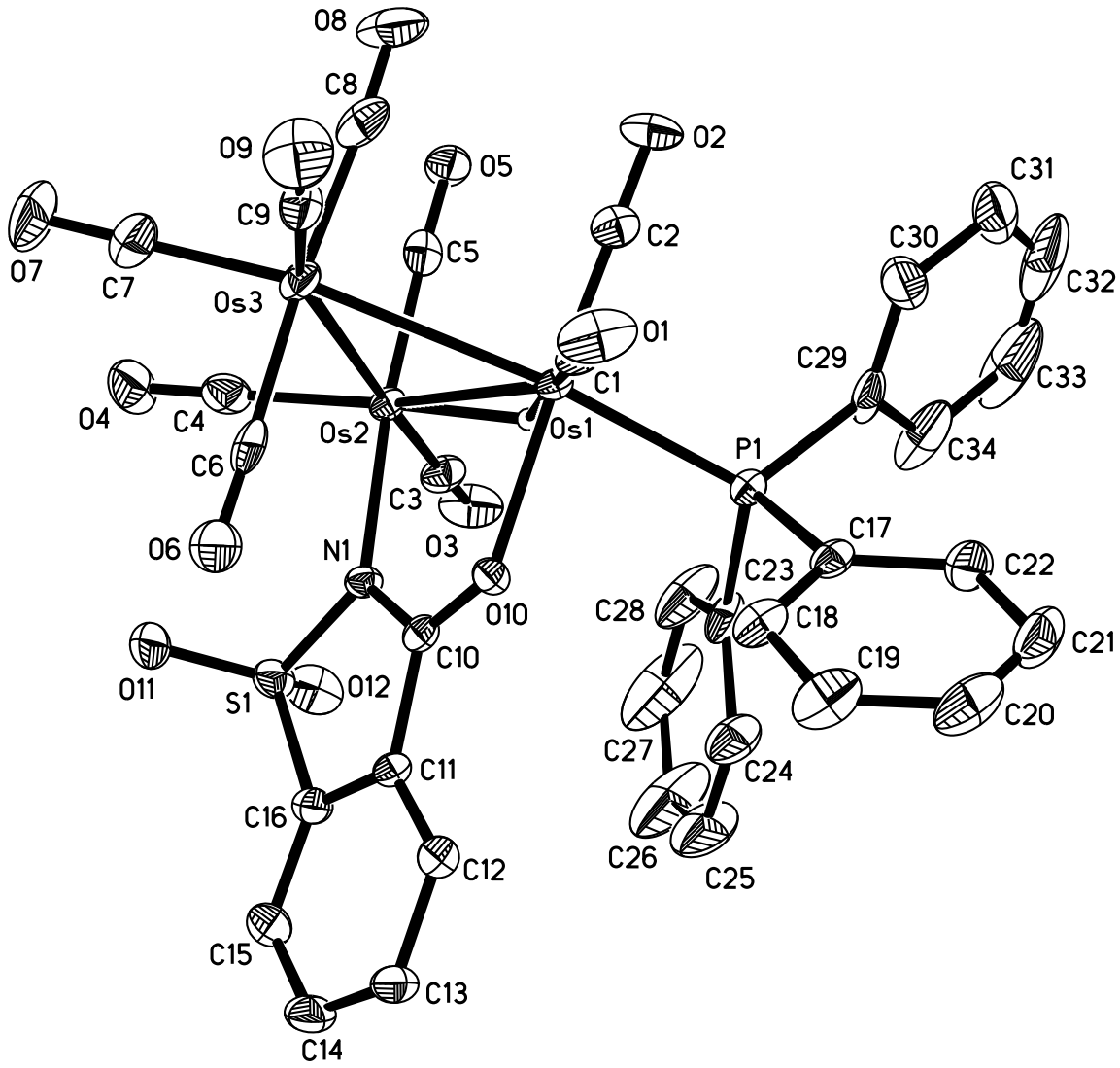

Fig. 2. The solid-state molecular structure of $Os_3(CO)_9(PPh_3)(\mu\text{-}H)(\mu\text{-}sac)$ (**2a**), showing 50% probability thermal ellipsoids. Ring hydrogen atoms were omitted for clarity. Selected interatomic distances (Å) and angles (°): Os(1)–Os(2) 2.9530(2), Os(1)–Os(3) 2.8982(3), Os(2)–Os(3) 2.8989(3), Os(1)–O(10) 2.158(3), Os(2)–N(1) 2.153(4), Os(1)–P(1) 2.3704(12), Os(2)–Os(1)–Os(3) 59.390(6), Os(1)–Os(2)–Os(3) 59.364(6), Os(1)–Os(3)–Os(2) 61.246(6), O(10)–Os(1)–Os(2) 82.40(8), O(10)–Os(1)–Os(3) 93.23(8), O(10)–Os(1)–P(1) 81.77(9), O(10)–Os(1)–C(1) 91.13(16), O(10)–Os(1)–C(2) 175.91(17), N(1)–Os(2)–Os(1) 79.77(10), N(1)–Os(2)–Os(3) 92.31(10), N(1)–Os(2)–C(3) 89.09(17), N(1)–Os(2)–C(4) 93.07(17), N(1)–Os(2)–C(5) 174.41(17), P(1)–Os(1)–Os(2) 114.47(3), P(1)–Os(1)–Os(3) 172.76(3), P(1)–Os(1)–C(1) 95.06(15), P(1)–Os(1)–C(2) 95.11(16).

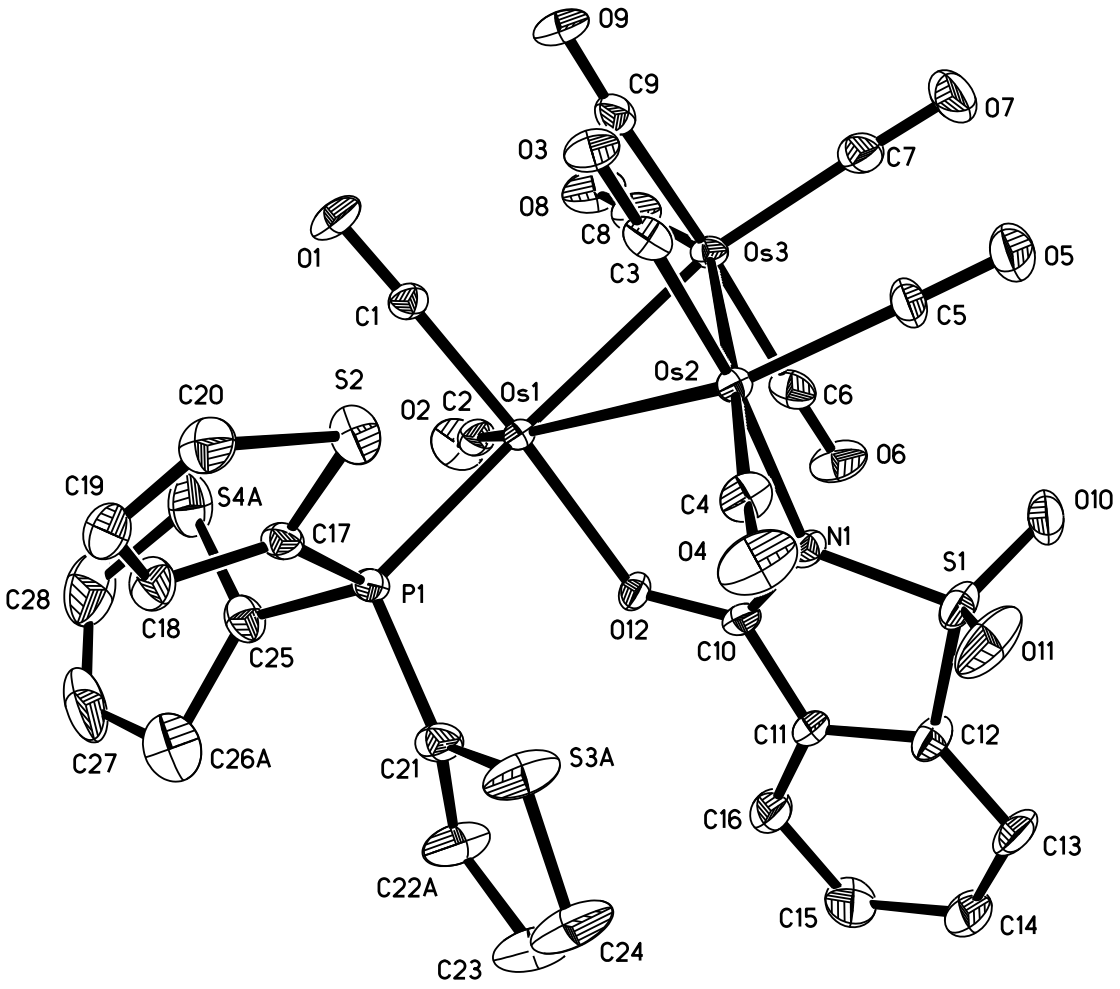

Fig. 3. The solid-state molecular structure of $Os_3(CO)_9(PTh_3)(\mu\text{-}H)(\mu\text{-}sac)$ (**2b**), showing 50% probability thermal ellipsoids for the major component of the disordered structure. Ring hydrogen atoms were omitted for clarity. Selected interatomic distances (Å) and angles (°): Os(1)–Os(2) 2.9541(3), Os(1)–Os(3) 2.8803(3), Os(2)–Os(3) 2.8734(3), Os(1)–O(12) 2.154(4), Os(2)–N(1) 2.143(5), Os(1)–P(1) 2.3428(16), Os(2)–Os(1)–Os(3) 58.993(8), Os(1)–Os(2)–Os(3) 59.221(8), Os(1)–Os(3)–Os(2) 61.786(8), O(12)–Os(1)–Os(2) 82.07(12), O(12)–Os(1)–Os(3) 94.60(12), O(12)–Os(1)–P(1) 86.60(13), O(12)–Os(1)–C(1) 175.4(2), O(12)–Os(1)–C(2) 84.8(2), N(1)–Os(2)–Os(1) 79.92(14), N(1)–Os(2)–Os(3) 89.56(15), N(1)–Os(2)–C(3) 174.2(2), N(1)–Os(2)–C(4) 87.7(2), N(1)–Os(2)–C(5) 93.6(3), P(1)–Os(1)–Os(2) 110.86(4), P(1)–Os(1)–Os(3) 169.37(4), P(1)–Os(1)–C(1) 91.5(2), P(1)–Os(1)–C(2) 99.6(2).

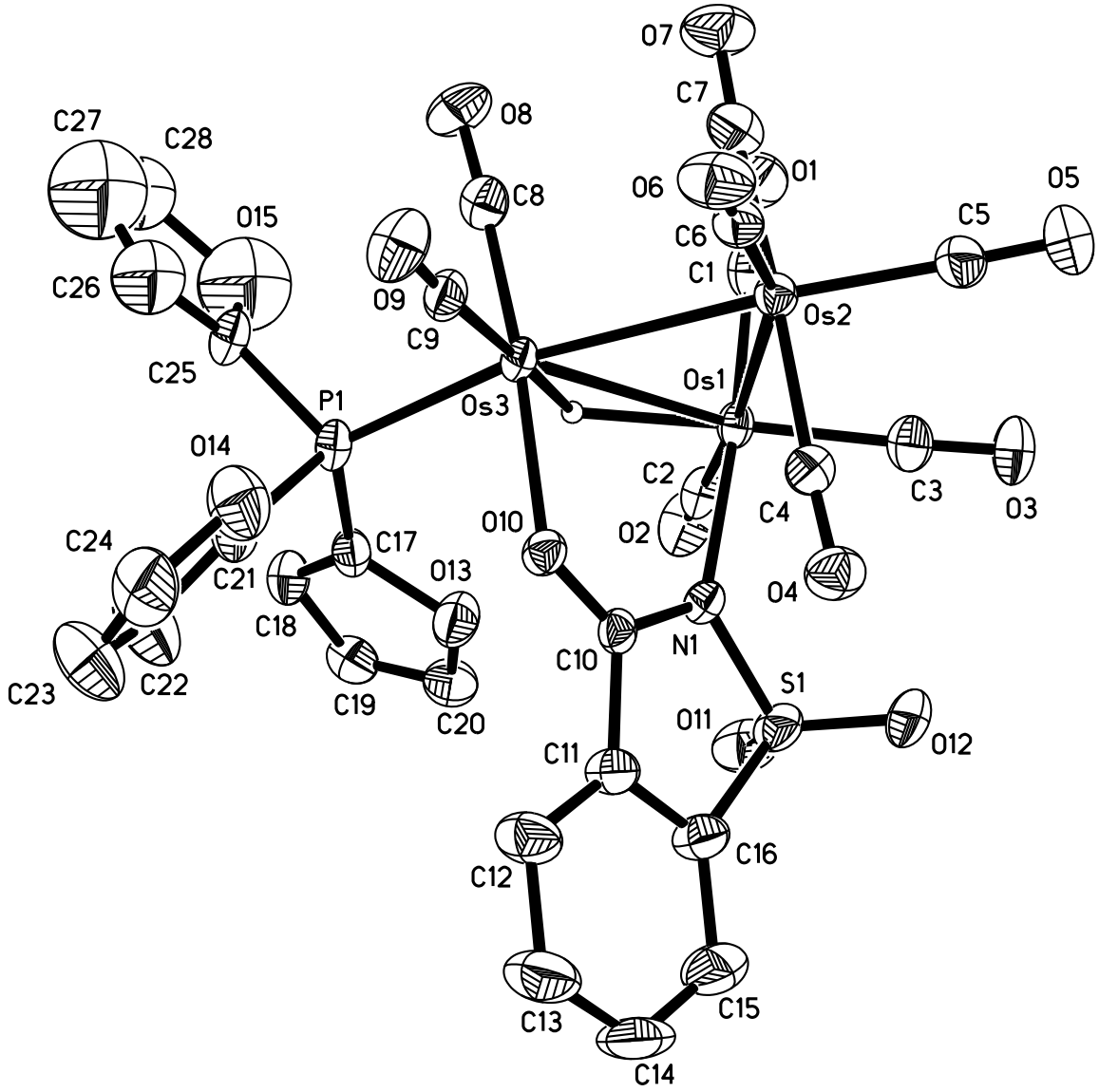

Fig. 4. The solid-state molecular structure for one of the two crystallographically unique, but chemically indistinguishable, molecules of $Os_3(CO)_9(PFu_3)(\mu\text{-H})(\mu\text{-sac})$ (**2c**), in the asymmetric unit, showing 50% probability thermal ellipsoids. Ring hydrogen atoms were omitted for clarity. Selected interatomic distances (Å) and angles (°): Os(1)–Os(2) 2.8755(3), Os(1)–Os(3) 2.9567(3), Os(2)–Os(3) 2.8670(3), Os(3)–O(10) 2.154(4), Os(1)–N(1) 2.158(4), Os(1)–P(1) 2.3419(14), Os(2)–Os(1)–Os(3) 58.869(7), Os(1)–Os(2)–Os(3) 61.978(7), Os(1)–Os(3)–Os(2) 59.153(7), O(10)–Os(3)–Os(1) 82.76(9), O(10)–Os(3)–Os(2) 89.07(9), O(10)–Os(3)–P(1) 82.35(10), O(10)–Os(3)–C(8) 174.9(2), O(10)–Os(3)–C(9) 92.84(19), N(1)–Os(1)–Os(2) 91.95(11), N(1)–Os(1)–Os(3) 79.55(11), N(1)–Os(1)–C(1) 174.7(2), N(1)–Os(1)–C(2) 90.6(2), N(1)–Os(1)–C(3) 94.4(2), P(1)–Os(3)–Os(1) 113.52(3), P(1)–Os(3)–Os(2) 169.56(4), P(1)–Os(3)–C(8) 92.53(18), P(1)–Os(3)–C(9) 95.97(17).

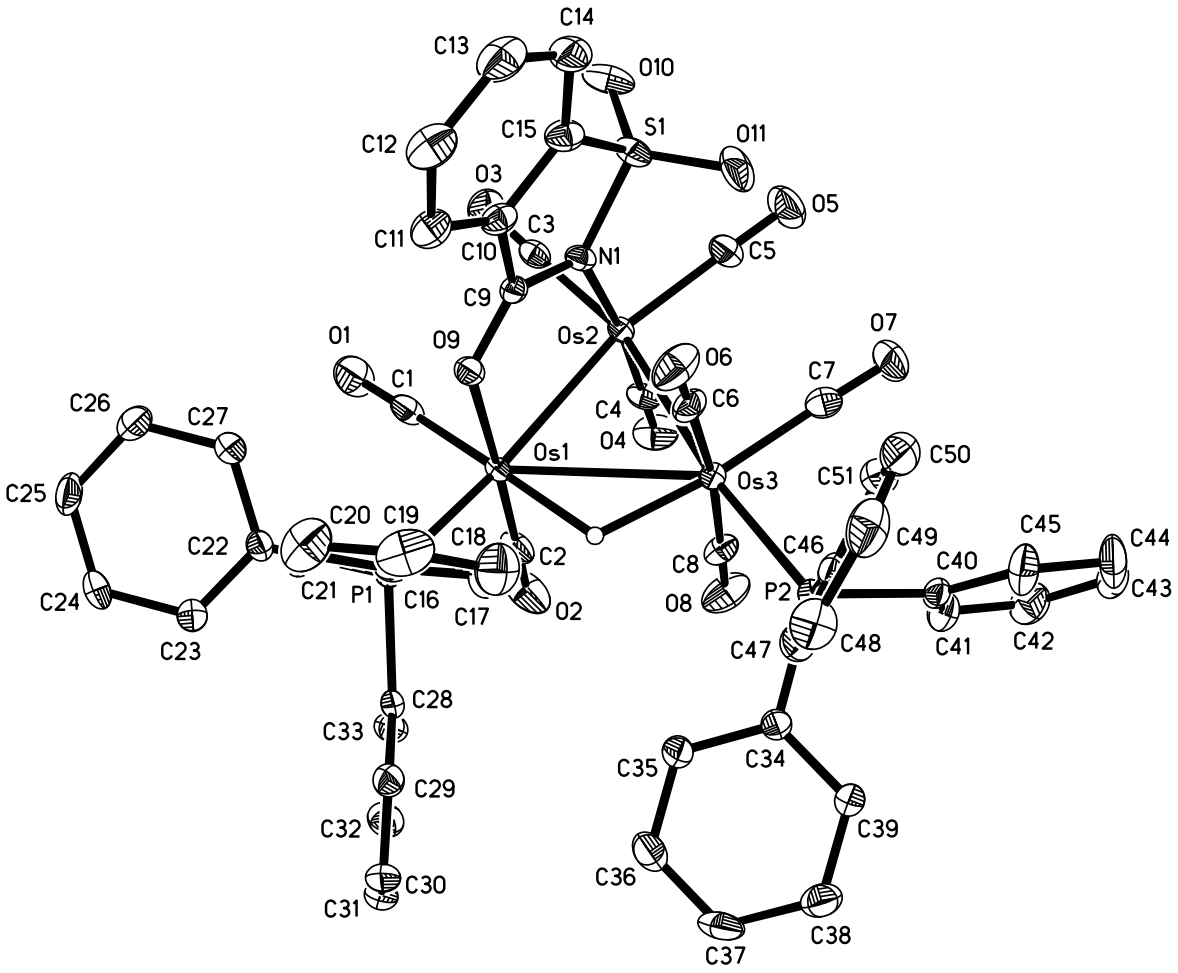

Fig. 5. The solid-state molecular structure of $Os_3(CO)_8(PPh_3)_2(\mu\text{-H})(\mu\text{-sac})$ (**3a**), showing 50% probability thermal ellipsoids. Ring hydrogen atoms were omitted for clarity. Selected interatomic distances (Å) and angles (°): Os(1)–Os(2) 2.78865(18), Os(1)–Os(3) 3.06618(18), Os(2)–Os(3) 2.89546(17), Os(1)–O(9) 2.170(2), Os(2)–N(1) 2.140(2), Os(1)–P(1) 2.3881(8), Os(3)–P(2) 2.3756(8), Os(2)–Os(1)–Os(3) 59.052(4), Os(1)–Os(2)–Os(3) 65.258(5), Os(1)–Os(3)–Os(2) 55.690(4), O(9)–Os(1)–Os(2) 84.44(5), O(9)–Os(1)–Os(3) 89.84(5), O(9)–Os(1)–P(1) 82.72(6), O(9)–Os(1)–C(1) 91.10(11), O(9)–Os(1)–C(2) 178.38(12), N(1)–Os(2)–Os(1) 82.01(7), N(1)–Os(2)–Os(3) 87.32(6), N(1)–Os(2)–C(3) 87.57(11), N(1)–Os(2)–C(4) 173.77(12), N(1)–Os(2)–C(5) 94.94(12), P(1)–Os(1)–Os(2) 166.79(2), P(1)–Os(1)–Os(3) 117.702(19), P(1)–Os(1)–C(1) 96.16(10), P(1)–Os(1)–C(2) 96.09(10), P(2)–Os(3)–Os(1) 131.11(2), P(2)–Os(3)–Os(2) 173.20(2), P(2)–Os(3)–C(6) 88.78(9), P(2)–Os(3)–C(7) 91.02(10), P(2)–Os(3)–C(8) 91.23(9).